Technical Report

UDC 621 . 771 . 23 : 62 - 523

Set-up and Control Technology of Nippon Steel & Sumitomo Metal Corporation Intelligent Mill

Shigeru OGAWA*
Takayuki OTSUKA
Kunihiko WAKATSUKI
Koichiro TAKESHITA
Daisuke NAKAGAWA
Kenji YAMADA
Tsuyoshi INOUE
Kenji SORAO
Keishiro IKEDA

Abstract

Operational scheme and flatness control algorithm with related mathematical models are developed for OPL (Oita Plate Leveler) which is a large scale embodiment of the NSSMC Intelligent Mill (NIM); NIM is a new concept rolling mill which can estimate and control roll force distribution across the width acting between the work roll (WR) and the rolled material. For zero adjustment procedure of individual position control system of divided back-up rolls (BURs), force distribution of the BURs minimizing the WR horizontal deflection is calculated by means of Lagrange's method of undetermined multipliers, and systematic way of realizing the target BUR force distribution is developed. Considering plan view inclination and temperature distribution of inlet material, flatness control algorithm is developed and practiced to obtain desired flatness as well as residual stress of the rolled material after cooling. Concluding research and development of NIM, contributions to flatness control theory for flat products and future tasks are pointed out.

1. Introduction

With the conventional method of flatness control used in the rolling of steel, sufficient control accuracy cannot be secured with the computer set-up capability alone, partly because of the requirement of a very high level of accuracy of control in the plate thickness distribution.[1)] For this reason, it is necessary to measure any flatness irregularities with a flatness detecting device behind the rolling mill and feed them back to a flatness control device. In the case of a system with such mechanisms, the transfer time of the material from the mill to the flatness detecting device constitutes a dead time in the flatness control system. This means that a flatness defect remains in the material that has been rolled from the time a flatness irregularity occurs until the time it is corrected. In addition, in many cases, the dead time prevents a quick response in control, making it difficult to implement sufficient flatness control. Under these conditions there is not only a decline in yield but also a deterioration in productivity because of the need for an extra process for correcting flatness irregularities.

With the aim of completely solving the above problems with the conventional rolling system, an intelligent mill based on an entirely new concept, that is, a mill incorporating a flatness detecting function, has been proposed,[2)] and a flatness detection and control system equipped with a rolling force distribution estimation capability has been demonstrated using a prototype mill comparable in size to a commercial strip mill.[3)] In addition, with the aim of enhancing productivity and function of the flatness correcting process of a plate conditioning line, hardware for the application of the intelligent mill as the Oita plate leveler (OPL) having a maximum rolling width of 5 500 mm was studied and has been developed into commercial production equipment.[4)]

Since the intelligent mill is entirely different in concept from conventional mills, conventional mill set-up and control techniques cannot be applied to it. In this technical report, we describe the operating software and set-up and control technology that have been developed exclusively for the intelligent mill and installed in the OPL.[5)]

* Executive Advisor, Dr.Eng.
20-1 Shintomi, Futtsu City, Chiba Pref. 293-8511

Table 1 Rolling conditions for OPL

Item		Specification
Plate size	Thickness	10–65 mm
	Width	1400–5500 mm
	Length	6–63.5 m
Plate temperature		R.T. −250 °C
Reduction		0.2 %
Rolling speed		10–120 m/min
Control interval		30 ms

Table 2 Roll dimensions of OPL

	WR	BUR (×19)
Diameter (mm)	330	550
Barrel length (mm)	6010	320
Chock span (mm)	6690	-

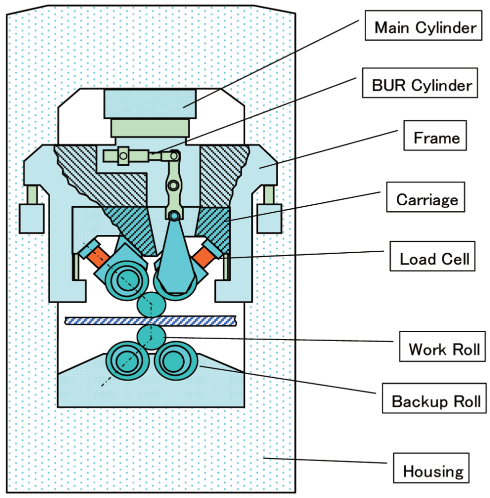

Fig. 1 Schematic view of OPL

2. Principal Equipment and Specifications of OPL[4)]

Table 1 shows the rolling conditions for the OPL. The plates to be leveled are 10–65 mm in thickness, 1400–5500 mm in width, and 6.0–63.5 m in length. The OPL is installed at the most upstream point of the shearing line of the plate mill of Oita Works of Nippon Steel & Sumitomo Metal Corporation, and it levels plates coming from the cooling bed by rolling them with an extremely light reduction of 0.2%. The OPL roll dimensions are shown in **Table 2**, and the basic construction of the OPL is shown in **Fig. 1**. The intelligent mill adopted as the OPL has the capability to estimate and control the rolling force distribution between the material being rolled and the work roll (WR) in real time. Since the rolling force distribution strongly reflects the flatness of the plate being rolled, the intelligent mill is capable of detecting and controlling the plate flatness without a time lag. This is the salient characteristic unique to the intelligent mill.

The WR has a diameter of 330 mm and a barrel length of 6010 mm. Each of the upper back-up rolls (BURs) is segmented type, 550 mm in diameter, and equipped with a load cell for estimating rolling force distribution. A total of 19 BURs—9 on the entry side and 10 on the delivery side—are arranged in a checker pattern at a cluster angle of 41°. In addition, for the purpose of flatness control, the upper segmented BURs are equipped with an individual hydraulic servo reduction control mechanism that adjusts the position of each BUR through the angle of the individual eccentric roll shaft. This BUR position defined in the normal direction common to the BUR and the upper WR is called an operating position. The entry- and delivery-side segmented BURs, each having a barrel length of 320 mm, are arranged across the width at a pitch of 295 mm. The maximum force of each segmented BUR is 2.74 MN, and the maximum rolling force in the vertical direction of the entire mill is 37.2 MN.

The lower BURs are arranged in vertical symmetry with the upper BURs. Since the flatness detection and control functions are performed exclusively by the upper BUR system, the lower BURs are equipped with neither load cells nor independent reduction capability. However, the entry- and delivery-side lower BURs have the capability to compensate for deflection of the lower WR by means of a pair of common eccentric shafts.

3. Development of OPL Set-up and Control Technology

3.1 Zero-point adjustment capability for segmented BUR positions

In the case of conventional cluster-type rolling mills, like the Sendzimir mill, the segmented BURs that are arranged across the width have a common shaft,[6)] which serves as the reference for the BUR positions. Therefore, the zero-point adjustment of segmented BUR positions is unnecessary. For the OPL, on the other hand, arranging a common shaft is not allowed because the upper BUR system is required to accurately measure the force applied to each of the segmented BURs. Needless to say, the segmented BURs arranged widthwise are designed and fabricated in such a way that their positions relative to WR become the same. However, since not only the individual eccentric roll shafts but also the chocks supporting them and the load cells are all separately arranged, their dimensional errors accumulate, causing positional error of each individual segmented BUR.

Therefore, for the OPL, it was decided to implement a zero-point adjustment of the position of each segmented BUR by kiss roll tightening, like the zero-point adjustment of screw-down in a 4- or 6-high mill. In the case of a 4-high mill, etc., screw-down devices on both the work side (WS) and the drive side (DS) are tightened with equal force. For the intelligent mill too, it was considered a basic requirement to apply a uniform force to each of the segmented BURs. However, in the case of the OPL, which has 9 entry-side segmented BURs and 10 delivery-side segmented BURs arranged in a checker pattern, if an equal force is applied to all the segmented BURs, the horizontal force acting upon the WR cannot be balanced. Thus, it is impossible to apply such a force to the BURs. Therefore, we first considered dividing the total BUR load into two equal parts and applying each part to the segmented BURs on the entry side and delivery side, respectively. For example, by applying a force of 980 kN to each of the entry-side BURs and a force of 882 kN to each of the delivery-side BURs, it becomes possible to apply a total load of 17.64 MN to the WR while keeping the horizontal forces acting on the WR in equilibrium.

Applying a uniform force to the entry side and the delivery side as mentioned above was intuitively decided with consideration given only to balancing the horizontal force acting upon the WRs. On the other hand, when a WR having a barrel length much larger than a diameter is used, as in the OPL, there is a possibility that the hori-

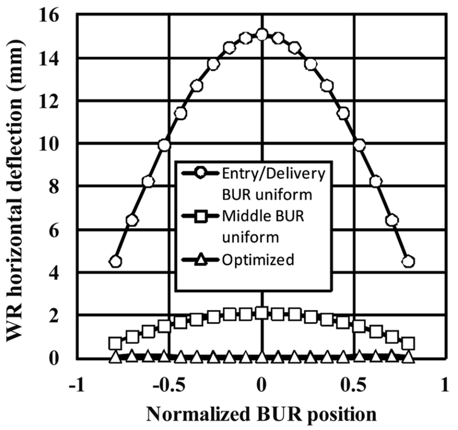

Fig. 2 WR horizontal deflection for OPL with total BUR force 17.64 MN

zontal deflection of the WR should become excessively large. Therefore, we calculated the horizontal deflection of the WR under the load mentioned above. The calculation results are shown in **Fig. 2**. It can be seen that the WR horizontal deflection is as large as 15 mm at the center. In the figure, the horizontal axis represents the center position of each segmented BUR normalized by 1/2 of the chock span of the WR. The horizontal deflection of 15 mm translates into 0.34 mm in terms of roll gap error, which is not negligible from the standpoint of the flatness control.

Therefore, we considered decreasing the WR horizontal deflection at the time of zero-point adjustment of the OPL segment BUR positions by adjusting the segmented BUR force distribution. The reason why a large WR horizontal deflection occurs when an equal force is applied to the entry- and delivery-side BURs, as shown in Fig. 2, is that, when 980 kN is applied to each entry-side segmented BUR and 882 kN is applied to each delivery-side segmented BUR, the entry side is always larger in horizontal force at any section cut out from the center of the WR barrel.

Therefore, we considered a new force distribution pattern in which, with the force applied to each of the 9 entry-side segmented BURs kept unchanged from 980, 490, or one-half of 980 kN, is applied to each of the two segmented BURs at the extreme ends, whereas 980 kN is applied to each of the other eight delivery-side segmented BURs. With this force distribution pattern, the total load on the entry side becomes equal to that on the delivery side, and the horizontal force applied to any section cut out from the WR center remains nearly the same. It was expected, therefore, that the horizontal deflection of the WR would decrease. The calculation results are also shown in Fig. 2. As expected, the new force distribution pattern decreased the WR horizontal deflection to about 2 mm. However, since the OPL that is intended to level rolled products is required to control the flatness of the material being rolled from the leading end, a further decrease in the WR horizontal deflection during the zero-point adjustment was desired.

Therefore, we considered obtaining theoretically the segmented BUR force distribution that minimizes the WR horizontal deflection. Denoting the force applied to i-th segmented BUR as q_i, q_i must satisfy the following equation since the WR horizontal force and moment are in equilibrium, as already mentioned:

$$T_i^x q_i = 0, \quad z_i T_{(i)}^x q_i = 0 \tag{1}$$

where, $T_i^x = \cos\theta_i$ (θ_i: angle of the direction of common normal of i-th segmented BUR and WR, as viewed counterclockwise from the x-axis defined by the rolling direction) and z_i is the z-coordinate (with the mill center as the origin) that indicates the position of the center of i-th segmented BUR across the width. In this paper, the summation convention for repeated indices is adopted; however, it is ignored for subscripts enclosed in parentheses.

When making an attempt to obtain the segmented BUR forces that minimize the WR deflection from the reference segmented BUR forces, $\bar{q}_i$, which are the segmented BUR forces obtained intuitively as described earlier, care should be taken that the total vertical force and moment acting on the WR remain unchanged. The segmented BUR forces to be obtained, q_i, must satisfy the following equation with T_i^y defined as $\sin\theta_i$:

$$T_i^y q_i = T_i^y \bar{q}_i, \quad z_i T_{(i)}^y q_i = z_i T_{(i)}^y \bar{q}_i \tag{2}$$

Next, we introduce the conditions for minimizing the horizontal deflection of the WR. Denoting the WR deformation matrix given by the beam bending theory[7,8] as K_{ij}^{WT}, the upper WR horizontal deflection, x_i^{WT} due to the segmented BUR forces, q_i, is given by the following equation:

$$x_i^{WT} = -K_{ij}^{WT} T_{(j)}^x q_j \tag{3}$$

As the basis of evaluation of the WR deflection, the straight line connecting the x-direction position of the No. 1 segmented BUR and that of No. N segmented BUR ($N=19$) is used to define the relative value of the WR horizontal deflection from the reference line described by the following equation:

$$\left[K_{ij}^H - \left(a_i K_{1j}^H + b_i K_{Nj}^H\right)\right] \cdot q_j \tag{4}$$

where, $K_{ij}^H = K_{ij}^{WT} T_{(j)}^x$, $a_i = (z_N - z_i)/(z_N - z_1)$, $b_i = (z_i - z_1)/(z_N - z_1)$.

Minimizing the absolute value of the relative value of WR deflection given by Equation (4), and the difference between segmented BUR forces to be obtained and the reference ones under the constraint conditions given by Equations (1) and (2), constitutes a stationary problem of the following function F:

$$F = \frac{1}{2}\left[\bar{K}_{ij}^H q_j \bar{K}_{ij}^H q_k\right] + \frac{1}{2} w_i \left\{\left(q_i - \bar{q}_i\right) / \bar{q}_{(i)}\right\}^2 + \lambda_m \left(T_i^m q_i - Q^m\right) \tag{5}$$

where, $\bar{K}_{ij}^H q_j$ is a simplified expression of Equation (4), and $T_i^m q_i = Q^m$ ($m=1, 2, 3, 4$) are simplified expressions of Equations (1) and (2). In Equation (5), w_i in the second term of the right side is the weight coefficient for adjusting the fidelity of the segmented BUR forces to the reference ones, and λ_m ($m=1, 2, 3, 4$) represents Lagrange multipliers for introducing the constraint conditions to Equations (1) and (2). By solving the system of linear equations obtained from the stationary requirement for function F in Equation (5) with respect to q_i and λ_m, it is possible to determine the segmented BUR forces for restraining the WR horizontal deflection while using the reference segmented BUR forces as the base.

Using the above technique and assuming the uniform force distribution in the center mentioned earlier as the reference segmented BUR force distribution, we calculated the segmented BUR forces that minimize the WR horizontal deflection with the weight coefficient for the reference value assumed to be $w_i = 1.0$ ($i=2, \ldots, 18$), $w_1 = w_{19} = 0.03$. The WR horizontal deflections obtained are shown in Fig. 2, and the segmented BUR force distribution is shown in **Fig. 3**. As can be seen from Fig. 3, the segmented BUR force distribution that minimizes the WR horizontal deflection is less regular than the reference uniform force distribution in the center. However, the WR horizontal deflections shown in Fig. 2 are significantly small, with

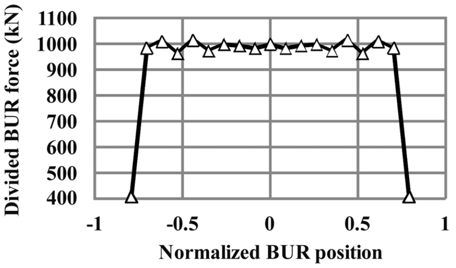

Fig. 3 Optimized BUR forces for zero adjustment procedure

even the maximum deflection only being approximately 0.13 mm, which translates into approximately 0.03 μm in terms of roll gap error. This level of error is negligible from the standpoint of flatness control.

Next, assuming the above force distribution as the target segmented BUR forces, q_i^0, during the zero-point adjustment of segmented BUR positions, we consider the method of attaining the target with the OPL.

First, with all the segmented BURs set in a mechanically neutral position, they are tightened with the main WS and DS screw-down device up to the total load (the sum of all BUR forces, 17.64 MN in the above example) while keeping the upper and lower WRs in contact with each other to obtain the current value of each of the segmented BUR forces, q_i ($i=1, \ldots, 19$). The main screw-down device is a hydraulic device that controls the vertical position of the entire upper frame supporting the upper BUR carriage as shown in Fig. 1.

Next, the zero-point adjustment force distribution, q_i^0, is attained by adjusting the operating positions of the segmented BURs. In so doing, even when the operating position of a specific segmented BUR is adjusted, forces of the other segmented BURs also change as a result of deflection of the WR and deformation of the carriage frame supporting the segmented BURs. Therefore, it is extremely inefficient to manually adjust the operating position of each of the 19 segmented BURs in order to attain the target force distribution qi0. Here, we developed an algorithm for attaining the target force distribution by adjusting all the segmented BUR positions simultaneously, giving due consideration to the OPL roll deformations, etc. The following modeling of OPL deformations has many things in common with the logic of flatness control described later. Therefore, we shall discuss it in detail here.

Denoting the operating position of each of the upper segmented BURs given by the individual servo reduction control mechanism as u_i and the force of each of the upper segmented BURs as q_i, the upper segmented BUR positions, u_i^{BT}, that reflect displacements of the upper segmented BURs in the normal direction common to the WR and BURs can be expressed by the following equation:[3)]

$$u_i^{BT} = K_{ij}^{BT}\left(q_j - q_j^0\right) - \left(u_i + U_i^0\right) \tag{6}$$

where, K_{ij}^{BT} denotes the deformation matrix of the upper segmented BURs, and U_i^0 denotes the absolute position of the segmented BURs under zero-point adjustment conditions ($u_i=0$, $q_i=q_i^0$). The method of identification of K_{ij}^{BT} and U_i^0 shall be described later.

The upper WR deflection, u_i^{WT}, in the normal direction common to the WR and the BURs is given by the following equation that combines horizontal deflection x_i^{WT} expressed by Equation (3) and vertical deflection y_i^{WT}:

$$u_i^{WT} = T_{(i)}^{x} x_i^{WT} + T_{(i)}^{y} y_i^{WT} \tag{7}$$

Denoting force distribution between the upper and lower WRs as p_i, vertical deflection of the upper WR, y_i^{WT}, can be calculated by using the following equation:

$$y_i^{WT} = K_{ij}^{WT}\left(p_j - T_{(j)}^{y} q_j\right) + c^y z_i + d^y \tag{8}$$

where, c^y and d^y denote the parameters of rigid body displacement of the WR in the vertical direction. The force distribution between the upper and lower WRs is determined by compatibility conditions between the upper and lower roll systems. Expressing the system of rolls from the lower roll assembly to the upper WR as an equivalent 2-high mill,[7)] and the roll deformation matrix of the equivalent 2-high mill as K_{ij}^{W}, Equation (8) can be rewritten as follows:

$$y_i^{WT} = -K_{ij}^{W} T_{(j)}^{y} q_j + f_i \tag{9}$$

The process by which Equation (9) was derived shall be explained in detail in the next section.

The displacement compatibility condition for the upper segmented BURs and upper WR is given by the following equation:

$$K_{ij}^{fT} q_j = u_i^{WT} - u_i^{BT} + C_i^{WT} \tag{10}$$

where, K_{ij}^{fT} denotes the roll flattening matrix,[9)] and C_i^{WT} denotes the upper WR profile.

From the above system of equations, changes in segmented BUR forces Δq_i when changes in operating positions of the segmented BURs Δu_i are given are obtained as follows. From Equation (6) for calculating the segmented BUR displacements, the changes in segmented BUR positions, Δu_i^{BT}, taking into account the changes in Δu_i and Δq_i, are calculated by using the following equation:

$$\Delta u_i^{BT} = K_{ij}^{BT} \Delta q_j - \Delta u_i \tag{11}$$

Substituting Equations (3) and (9) into Equation (7) to extract only the relative changes, the change in WR deflection, Δu_i^{WT}, is obtained by the following equation:

$$\Delta u_i^{WT} = -\left(T_{(i)}^{x} K_{ij}^{WT} T_{(j)}^{x} + T_{(i)}^{y} K_{ij}^{W} T_{(j)}^{y}\right)\Delta q_j \tag{12}$$

The relative value of the compatibility condition for the displacement between the upper WR and the BURs in Equation (10) can be expressed as follows:

$$K_{ij}^{fT} \Delta q_j = \Delta u_i^{WT} - \Delta u_i^{BT} \tag{13}$$

Substituting Equations (11) and (12) into Equation (13), the following relation between Δu_i and Δq_i is obtained:

$$\Delta u_i = \left(T_{(i)}^{x} K_{ij}^{WT} T_{(j)}^{x} + T_{(i)}^{y} K_{ij}^{W} T_{(j)}^{y} + K_{ij}^{BT} + K_{ij}^{fT}\right)\Delta q_j \tag{14}$$

Therefore, the segmented BUR displacements, Δu_i, for attaining the target zero-point adjustment force, q_i^0, from the current segmented BUR force, q_i, can be obtained by substituting $\Delta q_i = q_i^0 - q_i$ in Equation (14).

If the matrix in the parentheses of Equation (14), or the coefficient matrix for Δq_i on the right side of the equation, is accurate, the output of Δu_i obtained above would permit the attainment of the target zero-point adjustment force, q_i^0, by properly correcting the segmented BUR positions only once. Actually, however, since the matrix in parentheses is not completely free of error, and the mill deformation characteristics are not perfectly linear, there is little possibility that q_i^0 can be attained in a single attempt. On the other hand, even when the coefficient matrix of Δq_i contains errors, the segmented BUR forces positively come close to q_i^0 with the output of Δu_i calculated by using Equation (14). By repeating the process several times, it is possible to attain the target zero-point adjustment forces, q_i^0.

It should be noted that the zero-point adjustment of the segmented BUR positions must be carried out prior to the identification of mill deformation characteristics described later, for example, right after the installation of a new mill. At that time, the value of K_{ij}^{BT} in Equation (14) is unknown. Even in such a case, in the coefficient matrix of Δq_i in Equation (14), $T_{(i)}^{x} K_{ij}^{WT} T_{(j)}^{x}$ that expresses the deflection characteristics of a single WR is the most important element, which can be calculated from the WR dimensions alone. The other terms are: the equivalent 2-high deflection characteristics for the lower roll assembly and the upper WR combined; the upper segmented BUR deformation characteristics; and the roll-to-roll flattening deformation characteristics. However, since they are all high in stiffness as compared with the deflection stiffness of a single WR, they account for only a small proportion of the coefficient matrix of Δq_i in Equation (14).

Therefore, concerning the coefficient matrix of Δq_i excluding the upper WR deflection term, a fairly accurate approximate value can be obtained by, for example, roughly calculating only the diagonal terms from the stiffness at the time of total screw-down. In fact, by using such approximate values of the coefficient matrix, combined with the upper WR deflection term separately calculated based on the WR dimensions, the target zero-point adjustment forces, q_i^0, were attained by repeating the procedure of calculating Δu_i and correcting the segmented BUR positions five times or so. As a result, it has been made possible to keep the WR horizontal deflection within approximately 0.1 mm. In the case of the OPL, the control interval of the segmented BUR positions is 30 ms; therefore, correcting the BUR positions five times in succession takes only 150 ms. Thus, by using the above technique, it has become possible to implement accurately and speedily the set-up of the target zero-point adjustment forces that would take more than one hour if performed manually.

After the target zero-point adjustment forces are attained with the rolls kept in contact as described above, each segmented BUR operating position, u_i, is reset to 0, and the zero-point adjustment forces, q_i^0, are updated by using the current value of the segmented BUR forces, q_i, in order to completely eliminate error in the set-up of segmented BUR forces. As a result, u_i^{BT} in Equation (6) becomes $-U_i^0$, and the value of U_i^0 can be calculated by using Equation (10). This is all for the procedure for zero-point adjustment of the segmented BUR positions.

3.2 Technique to identify deformation characteristics of upper segmented BURs

Here, we consider the method of identifying the upper segmented BUR deformation matrix, K_{ij}^{BT}, defined by Equation (6). The deformation matrix corresponds to the mill stiffness of an ordinary mill and can be interpreted as mill deformation characteristics expressed in the form of a matrix by a segmented BUR configuration having independent load cells and position control mechanisms. As in the case of the ordinary mill stiffness, the deformation matrix is determined as the total deformation including not only the segmented BUR deformation, but also the deformation of the members that are subject to the roll force: bearings of BURs, load cells, carriages, frame, housing, etc. Since the deformation matrix reflects the deformation characteristics of the individual members, it is impossible to determine it theoretically and accurately on the basis of design data. Instead, it should be identified by means of a kiss roll tightening test.

In the case of the prototype intelligent mill,[3] the segmented BUR operating positions are manipulated independently with the kiss roll tightened to measure positions and forces of the individual segmented BURs. And by way of modeling the system of rolls from the lower roll assembly to the upper WR as an equivalent 2-high mill, the absolute positions of the upper segmented BURs in contact with the upper WR can be obtained. That way, the deformation matrix, K_{ij}^{BT}, was identified.[3] Thus, since the lower BUR of the prototype mill was a solid roll that could be modeled as a beam supported at both ends, the deformation characteristics of the upper segmented BURs could be identified with the lower BUR as the base. For the OPL, both the lower and upper BUR systems use segmented rolls whose deformation characteristics are unknown. Therefore, it is impossible to identify the deformation matrix of the upper BURs with the lower BURs as the base.

However, even when the deformation characteristics of the lower segmented BURs are unknown, if the upper WR deflection can be calculated, it is possible to identify the upper segmented BUR deformation characteristics. The upper WR horizontal deflection can be calculated by using Equation (3), and the upper WR vertical deflection can be calculated by using Equation (8). However, the force distribution between the upper and lower WRs, p_i, on the right side of Equation (8) is unknown. The value of p_i is determined from the compatibility condition between the upper and lower WR that is given by the following equation:

$$K_{ij}^{f} p_j = y_i^{WB} - y_i^{WT} + C_i^{WT} + C_i^{WB} \tag{15}$$

where, K_{ij}^{f} denotes the roll flattening matrix between the upper and lower WRs; C_i^{WB}, the lower WR profile; and y_i^{WB}, the lower WR deflection. Denoting the force distribution acting between the lower WR and the lower segmented BURs as r_i, the lower WR deflection can be calculated by using the following equation:

$$y_i^{WB} = K_{ij}^{WB} \left(T_{(j)}^{y} r_j - p_j \right) \tag{16}$$

Since the lower WR is in contact with the lower segmented BURs, Equation (16) naturally contains the rigid-body displacement component that corresponds to the deformation of the lower segmented BURs. Here, however, the rigid-body displacement component in Equation (16) shall be left out of consideration on the premise that the rigid-body displacement component attributable to the lower segmented BUR deformation is to be included in the upper segmented BUR deformation characteristics. Considering the OPL control algorithm in which not only the plate flatness control but also the plate thickness control is implemented with the upper segmented BURs as the only base, the above premise seems valid.

Now, it can be seen that when the values of r_i in Equation (16) are known, the equation is exactly the same as the equation for calculating the BUR deflection in an ordinary 4-high mill. Therefore, by incorporating segmented BURs having independent load cells like the upper segmented BURs as lower segmented BURs and subjecting it to a kiss roll tightening test as a special measure to identify the upper segmented BUR deformation characteristics, it is possible to measure r_i. This work procedure permits eliminating p_i from Equations (8) and (16) for calculating the WR deflection, and from Equation (15) for calculating the compatibility condition and thereby deriving Equation (9) for calculating the deformation matrix of an equivalent 2-high mill. As a result, it has become possible to adopt the same method of identifying the upper segmented BUR deformation characteristics as applied to the prototype mill.

3.3 Flatness control system

3.3.1 Basic algorithm of OPL flatness control

The basic algorithm of the OPL flatness control system is shown in **Fig. 4**. First, from measured operating positions u_i and forces q_i of the upper segmented BURs, using the segmented BUR deformation

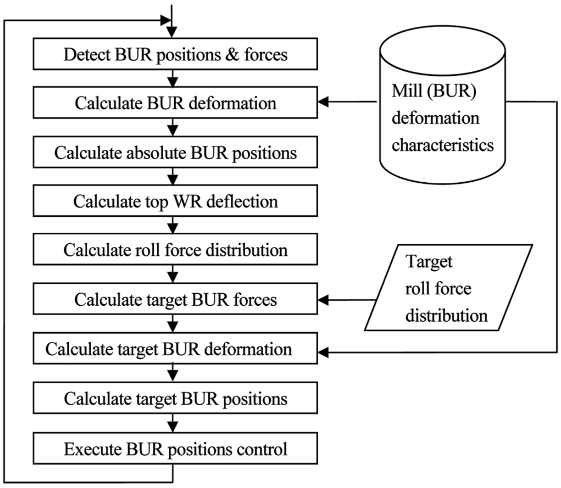

Fig. 4 Flatness control algorithm for OPL

characteristics, the segmented BUR deformation is calculated, and the absolute positions of the segmented BURs are determined from Equation (6). Next, the upper WR deflection, u_i^{WT}, is calculated from the WR-segmented BURs compatibility condition expressed by Equation (10). Then, the current value, p_i, of roll force distribution is obtained from the calculated upper WR deflection, u_i^{WT}, and the measured segmented BUR forces, q_i.

In short, by substituting Equations (3) and (8) into Equation (7), it is possible to obtain a system of equations for p_i and c^y, d^y. The roll force distribution, p_i, can be obtained by solving this system of equations together with the following equations of equilibrium of the upper WR vertical force and moment:

$$I_i\left(p_i - T^y_{(i)}q_i\right) + F_W^{\,y} + F_D^{\,y} = 0 \tag{17}$$

$$z_i\left(p_i - T^y_{(i)}q_i\right) + a\left(F_W^{\,y} + F_D^{\,y}\right)/2 = 0 \tag{18}$$

where, $F_W^{\,y}$ and $F_D^{\,y}$ denote, respectively, vertical WR bending forces on the work side (WS) and drive side (DS), with the force increasing side defined as positive; a, the WR span; and I_i, the vector whose components are all 1.

Next, a method of calculating the target value, q_i^G, of segmented BUR force distribution for attaining the target roll force distribution, p_i^G, shall be described in detail. The target roll force distribution, p_i^G, is a uniform distribution across the width. As described later, when consideration is given to thermal strain compensation by temperature distribution of the material being leveled and the deformation resistance distribution, p_i^G naturally becomes a non-uniform distribution. The target value, q_i^G, of segmented BUR force distribution is decided in a way to attain p_i^G and the target value, y_i^G, of the upper WR vertical deflection that corresponds to p_i^G. The following equation is used to calculate the upper WR vertical deflection:

$$K_{ij}^{WT}T^y_{(j)}q_j^G - c^y z_i - d^y = -y_i^G + K_{ij}^{WT}p_j^G \tag{19}$$

The equation shown above is obtained by substituting $y_i^{WT}=y_i^G$, $p_i=p_i^G$, and $q_i=q_i^G$ into Equation (8), which is used to calculate the upper WR deflection, and by moving the terms containing unknowns to the left hand side of the equation. Here, the target value, y_i^G, of the upper WR vertical deflection is decided on the basis of the upper WR vertical deflection obtained in the process of calculation of the current value, p_i, of roll force distribution, with consideration given to the expected effect of the change from p_i to p_i^G on the roll deformation.

The target value, q_i^G, of the segmented BUR force distribution must satisfy not only Equation (19) but also the following equations of equilibrium of the upper WR forces and moments in horizontal and vertical directions:

$$I_i T^x_{(i)}q_i^G = F_W^{\,x} + F_D^{\,x} \tag{20}$$

$$z_i T^x_{(i)}q_i^G = a\left(F_W^{\,x} - F_D^{\,x}\right)/2 \tag{21}$$

$$I_i T^y_{(i)}q_i^G = I_i p_i^G + F_W^{\,y} + F_D^{\,y} \tag{22}$$

$$z_i T^y_{(i)}q_i^G = z_i p_i^G + a\left(F_W^{\,y} - F_D^{\,y}\right)/2 \tag{23}$$

where, $F_W^{\,x}$ and $F_D^{\,x}$ denote, respectively, WS and DS horizontal bending forces of the WR, with the force in the rolling direction defined as positive. By solving the system of equations (19) through (23) for q_i^G and c^y, d^y, it is possible to obtain the target value, q_i^G, of the segmented BUR force distribution.

After q_i^G is obtained, the amount of segmented BUR deformation is calculated using the segmented BUR deformation characteristics, the target segmented BUR operating positions, u_i^G, is determined, and the amount of control increments of segmented BUR positions, $\Delta u_i=u_i^G-u_i$, which are required to attain the target value, y_i^G, of the upper WR vertical deflection, are obtained. This is similar to the procedure in which the amount of control increments, Δu_i, of the segmented BUR operating positions for attaining the required Δq_i are calculated by using Equation (14) in the zero-point adjustment work. Finally, the segmented BUR position control is executed, with due consideration given to the control gain. This loop of flatness control is repeated as required.

3.3.2 Problem of centering accuracy for plate to be leveled, and measures to solve the problem

Centering accuracy for rolled plates delivered from the cooling bed to the OPL is insufficient; it sometimes happens that a rolled plate enters the OPL in an off-centered manner, with the trailing end deviating as much as 100 to 200 mm from the leading end. Since the maximum length of the plate is 63 m, it was judged unrealistic in terms of cost to install side guides to improve the accuracy of centering. Therefore, the OPL leveling system was built without installing any special devices for improving the centering accuracy. Specifically, the width and amount of off-center of the plate being leveled are measured constantly at the entry side of the OPL so as to permit the implementation of the flatness control of the plate while estimating the width and amount of off-center of the plate at the OPL roll positions. In the algorithm of flatness control explained in Section 3.3.1, the measured width and amount of off-center of the plate are first tracked to the OPL roll bite position and then reflected in the calculation of the current value, p_i, and the target value of p_i^G of the roll force distribution.

3.3.3 Capability to compensate for temperature distribution of rolled plate to be leveled

The OPL is installed on the delivery side of the cooling bed. Except when the cooling bed is started up after many hours of shutdown, plates to be leveled are hotter than room temperature when they reach the OPL. In addition, in many cases, the cooling bed surface shows an uneven temperature distribution since it has been exposed to heat from rolled plates of various sizes and temperatures. Generally speaking, therefore, rolled plates that have passed over the cooling bed also show uneven temperature distributions. Therefore, the OPL flatness control system must be capable of leveling rolled plates which have a variety of temperature distributions.

Suppose, in the leveling of a rolled plate having a temperature deviation across the width, the plate is completely leveled by the

OPL. Since the temperature distribution of the plate becomes uniform after the plate is cooled down to room temperature, the strain due to thermal expansion corresponding to the uneven temperature distribution during the leveling by the OPL is relieved. As a result, the uneven temperature distribution during the leveling remains in the plate in the form of a residual stress, or the plate reveals a flatness defect as it buckles. In order to avoid such troubles, we developed a flatness control system that measures temperature distribution of the plate being leveled at the entry side of the OPL and compensates for thermal strain corresponding to the temperature distribution in the OPL.

The linear expansion coefficient of the plate being leveled as is denoted as α, the width of the plate being leveled as b, the width of each of the widthwise elements obtained by dividing the plate width according to a set of barrel length of corresponding segmented BURs as Δz_i ($i = M_D, \ldots, M_W$), and the temperature obtained by averaging the temperature distribution of the plate being leveled by the element width as T_i. Then, the thermal strain distribution, $\Delta\varepsilon_i$, of the plate being leveled, with temperature T_R as the base, is given by the following equation:

$$\Delta\varepsilon_i = \alpha\left(T_i - T_R\right) = \alpha \cdot \Delta T_i \quad (24)$$

After the plate being leveled is cooled to room temperature, the widthwise integral average of the strain that is relieved under no external force must be zero. Namely, in Equation (24), T_R must be the integral average of T_i. Thus,

$$T_R = \Delta z_i T_i / b \quad (25)$$

It can be seen, therefore, that, in order to have a flat plate at room temperature, as the strain in Equation (24) (the strain shall hereafter be called the elongation difference, because it means the difference from the average value) is relieved, the plate should be leveled by giving the same elongation difference as that in Equation (24) by rolling during the OPL leveling operation.

As expressed by Equation (19), the OPL performs the flatness control by achieving the required roll force distribution, p_i^G. Therefore, when the purpose of the OPL is not to make the plate flat but to give the elongation difference, $\Delta\varepsilon_i$, expressed by Equation (24), it is only necessary to give the roll force distribution corresponding to that elongation difference as the target value to the OPL.

According to the theory of two-dimensional rolling, the rolling force per unit width, p_i, with the influence of rolling tension taken into account, can be calculated by using the following simple equation when the reduction in thickness is small:[10)]

$$p_i = Q_P \ell_d \left[k_i - \left\{\delta\sigma_{fi} + \left(1 - \delta\right)\sigma_{bi}\right\}\right] \quad (26)$$

where, Q_P denotes a pressure multiplication factor; ℓ_d is the projected contact arc length; k_i is the average deformation resistance; σ_{fi} is the delivery-side tension; σ_{bi} is the entry-side tension; and δ is a parameter determining the allocation of the influence of tension.

The elongation difference is correlated to the tension distribution through the theory of feedback effect by the following equation:[7)]

$$\sigma_{fi} = \sigma_{bi} = -E\Delta\varepsilon_i \quad (27)$$

where E denotes Young's modulus of a rolled plate, and the average tension is assumed to be 0. Substituting Equation (27) into Equation (26), and considering Equation (24), the following equation is obtained:

$$p_i = Q_P \ell_d \left[k_i + E\alpha\Delta T_i\right] \quad (28)$$

By adopting the p_i value given by Equation (28) as the target roll force distribution, p_i^G, to be used in Equation (19), it is possible to compensate for the thermal strain that occurs in the plate cooling process after the OPL leveling operation.

When considering the influence of temperature distribution of the plate being leveled in Equation (28), consideration should also be given to the influence of temperature on the average deformation resistance, k_i. It can be confirmed from the rolling forces actually observed in the OPL operation that, even in warm rolling, the temperature influences the deformation resistance of a plate being leveled. It has been found that within the OPL rolling temperature range, the relationship between the temperature and deformation resistance is almost linear. Specifically, denoting the deformation resistance corresponding to room temperature T_r as k_r, the deformation resistance, k_i, at a given temperature, T_i, is expressed by the following equation using influence coefficient, β:

$$k_i = k_r - \beta\left(T_i - T_r\right) \quad (29)$$

Therefore, the deformation resistance, k_R, at average temperature, T_R, of the plate being leveled can be calculated by using the following equation:

$$k_R = k_r - \beta\left(T_R - T_r\right) \quad (30)$$

The deformation resistance distribution, k_i, corresponding to the temperature distribution $\Delta T_i = T_i - T_R$ with T_R as the base is calculated by using the following equation, eliminating k_r from Equations (29) and (30):

$$k_i = k_R - \beta \cdot \Delta T_i \quad (31)$$

Substituting Equation (31) into Equation (28) gives the following equation:

$$p_i = Q_P \ell_d \left[k_R + E\left(\alpha - \frac{\beta}{E}\right)\Delta T_i\right] = Q_P \ell_d \left[k_R + E\bar{\alpha}\Delta T_i\right] \quad (32)$$

where $\bar{\alpha} = \alpha - \beta / E$; the value can be regarded as the linear expansion coefficient when consideration is given to the influence of temperature on the deformation resistance.

For example, if we consider a 20 mm thick steel plate having a yield stress of 350 MPa, when $\alpha = 1.30 \times 10^{-5}$/K, β/E was 0.45×10^{-5}/K from the OPL rolling force observation. Therefore, $\bar{\alpha} = 0.85 \times 10^{-5}$/K. Thus, it can be seen that the influence of temperature on the deformation resistance has the effect of easing the term for compensating for the thermal strain.

From the above, we have established that by measuring the temperature distribution of the plate to be leveled at the entry side of the OPL, feeding the measurement data to the OPL on a real-time basis, calculating by Equation (32) the target roll force distribution for the widthwise temperature distribution during rolling, and using it for flatness control, it becomes possible to compensate for the temperature distribution across the width and the influence of its change along the length.

4. Putting Real-Time Flatness Control Technology into Practical Use

The OPL set-up and control technology that has been described so far has been implemented in commercial production equipment. During rolling, the temperature distribution, width, and amount of off-center of the plate to be leveled are constantly measured at the entry side of the OPL. They are tracked to the roll bite and used as the data for flatness control. The OPL constantly measures the segmented BUR positions and forces and controls the segmented BUR positions at intervals of 30 ms using the flatness control algorithm shown in Fig. 4.

Figure 5 shows segmented BUR force distributions and roll force distributions measured when a 12 mm-thick, 5 200 mm-wide plate was leveled, at positions 0.5, 3.0, 5.4, 7.6, 10.0, and 12.4 m from the front end of the plate. The leveling of a plate by the OPL is performed by bending the WRs according to the plate thickness distribution and applying a uniform reduction in thickness to them across the width. Since the required bending moment is given to each individual WR position, the segmented BUR force distributions generally become uneven, as shown in Fig. 5 (a). On the other hand, the roll force distributions are almost uniform across the width, as shown in Fig. 5 (b). From those results, it is considered impossible for the OPL operator, for example, to manually adjust the segmented BUR positions while observing the segmented BUR forces directly. Thus, it can be understood that the automatic control theory and algorithm that have been described so far are indispensable for the OPL.

Incidentally, looking at the roll force distribution at a position 0.5 m from the front end of the plate shown in Fig. 5 (b), it can be seen that the roll force for the No. 1 segmented BUR on the drive side (DS) of the rolling line is zero. The reason for this is as follows. The rolled plate discharged from the cooling bed entered the OPL in an off-centered manner as described in Section 3.3.2 and, as a result, the plate that had not been under the No. 1 segmented BUR at the front end came under that roll when the plate moved 3.0 m. Thus, it has been confirmed that the flatness control is performed properly even when the plate to be leveled travels obliquely and crosses the boundary between segmented BURs.

Figure 6 shows changes in the amount of off-center of the above rolled plate, and in the WR vertical and horizontal bending forces. By definition, the amount of off-center toward the work side (WS) of the rolling line is positive. It can be seen from Fig. 6 that the plate moved obliquely from the WS toward the DS by about 100 mm. Similarly, the WR bending forces, especially the vertical bending forces on the WS and DS, changed in the opposite direction. The implication is that the WR bending forces properly complement the flatness control by the segmented BURs. Thus, in the case of a large-width plate, which covers the entire positions of the segmented BURs, the WR benders are effectively utilized in the flatness control. In this case, there exist a total of 23 equations to be satisfied—19 for Equation (19) and one for each of Equations (20) to (23). Therefore, it is possible to solve the system of Equations (19) through (23), with not only the segmented BUR force, q_i^G, but also the WR vertical and horizontal bending forces, F_W^x, F_D^x, F_W^y, F_D^y, as unknowns. Thus, the output for the control of the WR benders can be calculated simultaneously.

In order to study an effect of the capability to compensate for the temperature distribution of a plate being leveled as described in Section 3.3.3, the camber of each of four cut samples obtained from a thick plate was measured. The samples were collected as follows. The plate (thickness: 21.5 mm, width: 2 550 mm, yield stress: 350 MPa) was cooled to room temperature after it was leveled by the OPL. Then, the tail-end portion 10 m in length was cut out from the plate as shown in **Fig. 7**. After a left-hand portion 300 mm in width was cut off, four samples ((1), (2), (3), and (4)) were slit out from the tail-end portion of the plate. The reason why the 300 mm-wide samples ((1) and (3)) and the 150 mm-wide samples ((2) and (4)) were slit out alternately was to obtain measurement data independent of the pitch of the OPL segmented BURs, which are arranged at the pitch of 295 mm. The four samples were cut at the same time with multiple gas torches arranged across the plate width. With this slitting method, it had been confirmed in advance that there was very little possibility that the samples were subject to thermal strain unevenly during slitting procedure.

Figure 8 shows the results of measurement of the cambers of the slit-out samples. When the capability to compensate for the temperature distribution was not used (Fig. 8 (a)), the cambers measured

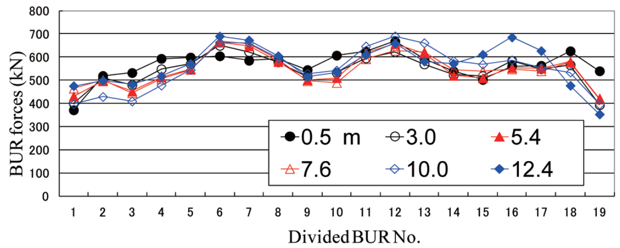

(a) Divided BUR forces

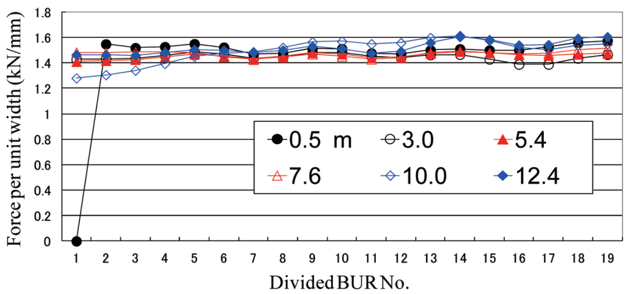

(b) Roll force distribution

Fig. 5 Result of control of roll force distribution (12 mm thickness × 5 200 mm width)

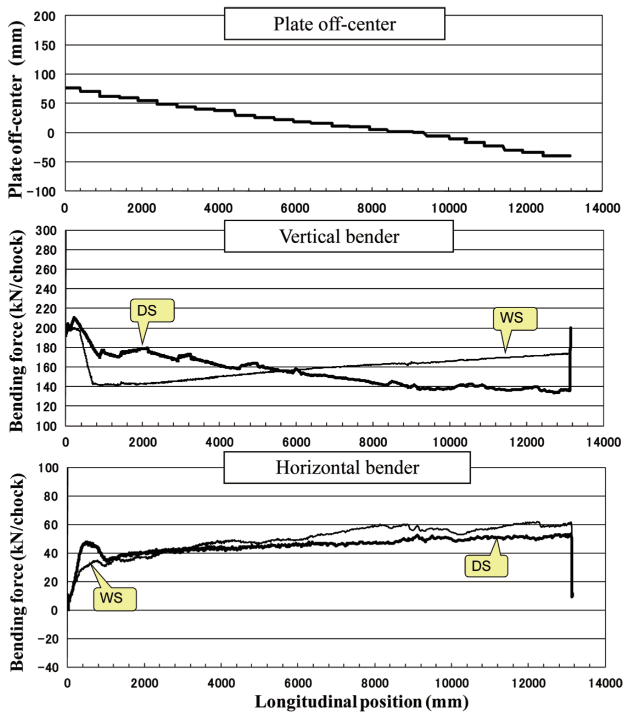

Fig. 6 Plate off-center and corresponding WR bender behavior (12 mm thickness × 5 200 mm width)

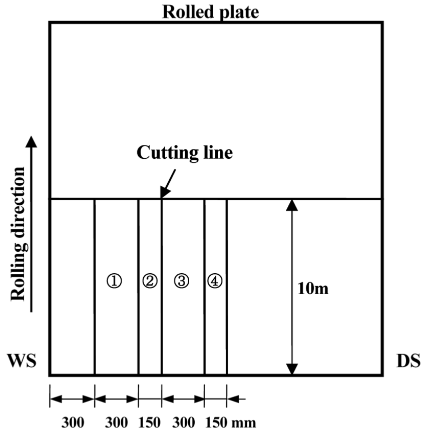

Fig. 7 Sampling description for residual stress measurement

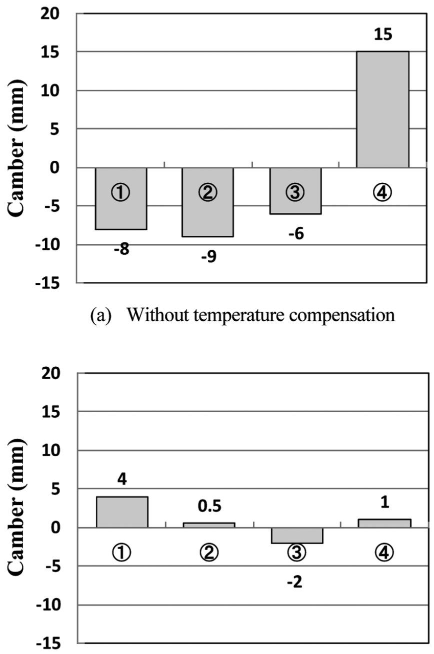

(a) Without temperature compensation

(b) With temperature compensation

Fig. 8 Cambers measured after slitting out samples

were about 10 mm per 10 m. On the other hand, when this capability was used in the flatness control (Fig. 8 (b)), the maximum camber measured was 4 mm. Therefore, it can be judged that the capability to compensate for the temperature distribution is effective. The occurrence of a camber with the slit-out samples is considered to be due to the widthwise distribution of a longitudinal residual stress that was present in the leveled plate. The fact that there are significant decreases in the camber of the slit-out samples implies that the residual stress in the rolled plate decreased after the plate was leveled by the OPL and cooled down to room temperature.

Figure 9 shows an example of plate flatness improvement by the OPL. Shown here are bird's-eye views of a longitudinally-profiled (LP) plate differing in thickness along the length, whose flatness was measured with a flatness detecting device set on the OPL delivery side.

The upper diagram in Fig. 9 shows the flatness of the LP plate that was not leveled by the OPL. Many LP plates have poor flatness

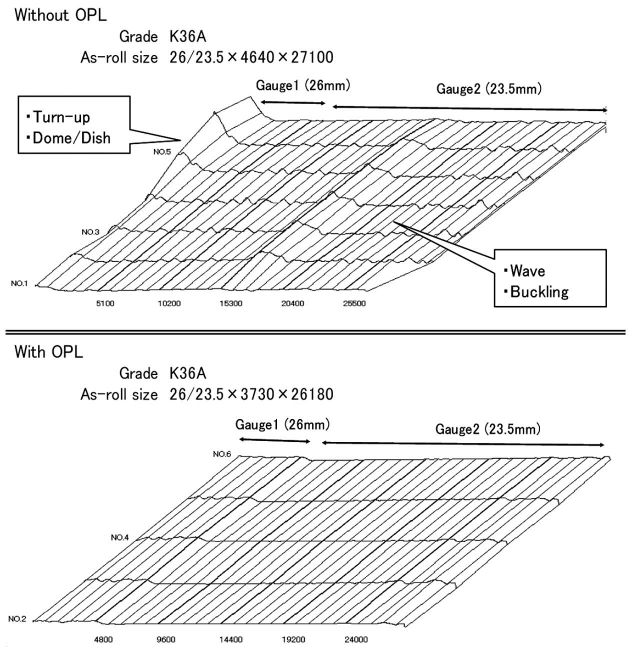

Fig. 9 Leveling performance for longitudinally profiled plate

when they are delivered from the cooling bed because of thickness variation. It is also not easy to level them with a cold roller leveler, because the bending strain given by the roller leveler inevitably varies due to the thickness variation of the plate along the length. On the other hand, the OPL levels the plate at a single point along the length right under the WR. Therefore, unlike the roller leveler, the OPL has no difficulty in leveling the LP plate along the whole length containing the thickness variation. As a result, as shown in the lower diagram in Fig. 9, the OPL can also effectively perform the flatness control of the LP plates.

5. Significance of R&D on the Intelligent Mill as Viewed from Rolling Theory and Tasks to Tackle in the Future

Our R&D on the intelligent mill has been brought to a conclusion as the OPL has been put into practical application as described herein. In this section, we shall discuss the significance of the R&D on the intelligent mill that has been carried out to date, especially from the standpoint of rolling theory on flatness control.

5.1 Significance of R&D on the intelligent mill as viewed from standpoint of flatness control theory

5.1.1 Influence of flatness of entry-side plate

It has been confirmed by laboratory experiments that in cold rolling, the flatness of a plate to be rolled on the entry side does not influence the flatness of the plate on the delivery side.[11)] In the theory of flatness control, on the other hand, it had been an important hypothesis that the flatness of a plate on the entry side does not influence the roll force distribution.[7)] We verified this hypothesis for the first time by means of the roll force distribution detection capability that is unique to the intelligent mill.

Concrete supporting data are shown in **Fig. 10**. The intelligent mill used was a pilot mill having WRs 80 mm in diameter and 7-segment BURs. Three mild steel sheets (thickness: 1 mm, width: 380 mm) having wavy edges, a flat surface, and center buckles, respectively, were rolled with a reduction in thickness of 2% with the segmented BUR positions kept unchanged. Under these conditions,

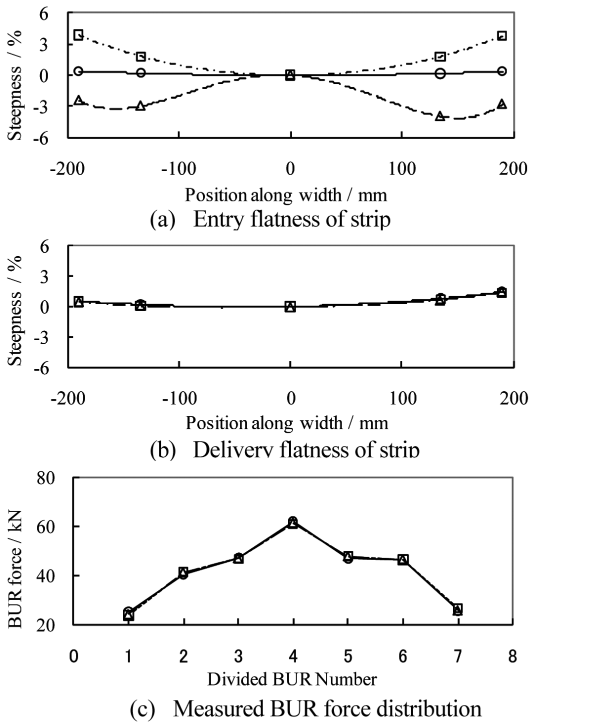

Fig. 10 Effect of entry strip flatness on delivery strip flatness and BUR force distribution obtained by NIM pilot mill [2]

the segmented BUR force distributions and flatness of the rolled sheets were measured. It can clearly be seen from Fig. 10 that regardless of the sheet flatness on the entry side, the sheet flatness on the delivery side and the segmented BUR force distribution remained almost unchanged.[2] As can be seen from the method of calculation of roll force distribution explained in Section 3.3.1, the fact that the segmented BUR positions and the segmented BUR force distributions remain unchanged indicates that the roll force distribution remains the same. From this result, it can be understood that sheet flatness on the entry side does not influence mechanical conditions within the roll bite.

With the intelligent mill, therefore, it is possible to obtain the desired sheet flatness on the delivery side without measuring the entry-side sheet flatness. Specifically, as long as the deformation resistance of the material being rolled is uniform across its width, the desired delivery-side flatness can be obtained, regardless of the entry-side flatness, by controlling the flatness aiming at uniform roll force distribution across the width.

5.1.2 Relationship between reduction in thickness (elongation) and entry-side flatness

In order to level a plate by removing the elongation difference from the entry-side plate by means of rolling, it is considered necessary to apply an elongation, or a reduction in thickness, which is larger than the elongation difference that exists in the form of a flatness defect in the entry-side plate. However, from the results of experiments with the intelligent mill, it was confirmed that a plate could be leveled even with an elongation smaller than the elongation difference corresponding to the entry-side flatness.

Figure 11 shows entry- and delivery-side steepness measured when a steel plate 8.9 mm in thickness and 1 635 mm in width was rolled with an elongation of 0.2% by a prototype intelligent mill having WRs 200 mm in diameter and 7-segment BURs. As shown,

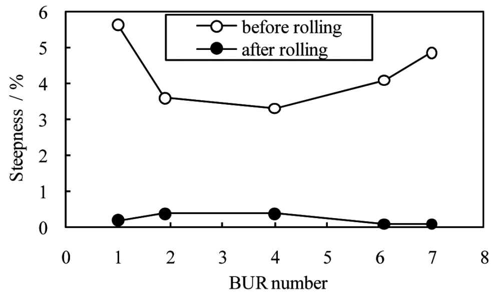

Fig. 11 Flatness of a rolled plate before rolling and after rolling rolled by NIM prototype mill [3]

by rolling with a small elongation the plate having a marked flatness defect (steepness exceeding 5%), it is possible to obtain a flat surface whose steepness is only about 0.3%.[3] Since the entry-side flatness also contained a swell (full wave) component, the net elongation difference calculated was about 0.4%. Specifically, the plate could be leveled satisfactorily by rolling it with an elongation of about 1/2 of the elongation difference corresponding to the entry-side flatness. The positional conditions for the segmented BURs of the intelligent mill were exactly the same as those for rolling a flat plate at the entry-side of the same size to obtain the same delivery-side flatness. These experimental results show that the principle that entry-side flatness influences neither delivery-side flatness nor roll force distribution applies even in rolling with an extremely small elongation.

With a conventional commercial mill for rolling a plate 1 000 mm or more in width, it is difficult to accurately control the mechanical plate crown to the same level as the entry-side thickness distribution of the plate. Therefore, rolling with an extremely light reduction, or an elongation of 0.2% or under, can hardly be implemented on a stable basis. The reason for this is as follows. When the reduction in thickness is small, the widthwise distribution that is unmatched between entry-side thickness distribution and roll gap distribution during rolling, or mechanical plate crown, becomes relatively large, preventing plastic deformation of a plate across the width as the reduction in thickness decreases. As a result, prescribed elongation cannot be secured. Therefore, it may be said that the fact that entry-side flatness does not influence delivery-side flatness even in rolling with an extremely light reduction could be confirmed for the first time by the intelligent mill's unique capability to detect and control roll force distribution.

This observation suggests that the leveling technology of the intelligent mill has an advantage over that of a roller leveler, especially when it comes to leveling high-tensile steel plates. Specifically, with a roller leveler, it is necessary to give a strain 3 to 5 times of the yield strain to the surface of a plate to be leveled in order to expand the through-thickness plastic deformation region to a certain extent. Since yield strain for a high-tensile steel plate is large, the deterioration of qualities becomes conspicuous when the plate is leveled. On the other hand, with the intelligent mill, the deterioration of material qualities caused by leveling is much less conspicuous since a plate can be leveled with an extremely light reduction regardless of yield strain of the plate.

5.1.3 Quantitative verification of feedback effect of tension

Since the intelligent mill is capable of directly controlling rolling force distribution on a real-time basis, it is possible to confirm correspondence between delivery-side flatness and rolling force distribution. The relation between the changes in rolling force distribution and those in delivery-side flatness are calculated by utilizing the theory of effect of tension feedback shown in Equation (27). It is verified by many results of rolling, including the capability to compensate for temperature distribution described in Section 3.3.3, that delivery-side flatness can be accurately controlled by way of Equation (27). Specifically, it is concluded that through our R&D on the intelligent mill, the hypothesis on the effect of tension feedback has been verified both quantitatively and qualitatively.

5.2 Problem relating to flatness control theory

As has been described above, through our R&D on the intelligent mill, it has been confirmed that entry-side flatness influences neither delivery-side flatness nor rolling force distribution, and that this holds true even in rolling with an elongation far smaller than the elongation difference corresponding to the entry-side flatness. The implication is that the elongation difference existing in a plate to be rolled in the form of entry-side flatness is removed almost completely at the roll bite entrance, and thus it does not influence mechanical conditions within the roll bite.

The above conclusion has been derived from circumstantial evidence based on the results of the rolling operations of the intelligent mill. We consider that verifying the above conclusion directly as a basic mechanism of rolling is an important theme in our future research on rolling theory.

6. Conclusion

We developed operating software and flatness control technology for putting into practical use a new-type of intelligent mill having the capability to detect and control flatness of a rolled plate termed as the OPL. As a result, we could come up with practical technology that permits accurately leveling rolled plates moving obliquely into the leveler from the cooling bed, rolled plates having an uneven temperature distribution, and even LP plates that differ in thickness along the length.

In addition, we discussed the advances in flatness control theory brought about by a successive series of R&D on the intelligent mill, and the tasks to tackle in the future.

References

1) Suzuki, H.: Journal of the Japan Society for Technology of Plasticity. 20 (217), 83 (1979)
2) Ogawa, S. et al.: Journal of the Japan Society for Technology of Plasticity. 52 (609), 1094 (2011)
3) Ogawa, S. et al.: Journal of the Japan Society for Technology of Plasticity. 52 (609), 1099 (2011)
4) Ogawa, S. et al.: The Iron and Steel Institute of Japan, Reference Material for 131st Rolling Theory Committee Meeting. Atsuri-131-14, 2009
5) Ogawa, S. et al.: Tetsu-to-Hagané. 100 (12), 1490 (2014)
6) Suzuki, H.: Journal of the Japan Society for Technology of Plasticity. 23 (263), 1123 (1982)
7) Matsumoto, H. et al.: Journal of the Japan Society for Technology of Plasticity. 23 (263), 1201 (1982)
8) The Japan Society for Technology of Plasticity: Handbook ofTechnology of Plasticity. Tokyo, Corona Publishing Co., 2006, p. 21
9) Tozawa, Y. et al.: Journal of the Japan Society for Technology of Plasticity. 11 (108), 29 (1970)
10) Rolling Theory Committee of the Iron and Steel Institute of Japan: Theory and Practice of Flat Rolling. Tokyo, Iron and Steel Institute of Japan, 1984, p. 36
11) Nakajima, H. et al.: Tetsu-to-Hagané. 59 (2), A33 (1973)

Shigeru OGAWA
Executive Advisor, Dr.Eng.
20-1 Shintomi, Futtsu City, Chiba Pref. 293-8511

Kenji YAMADA
Chief Researcher
Integrated Process Research Lab.
Process Research Laboratories

Takayuki OTSUKA
Senior Researcher, Ph.D.
Integrated Process Research Lab.
Process Research Laboratories

Tsuyoshi INOUE
Chief Researcher
Steel Rolling Research Lab.
Process Research Laboratories

Kunihiko WAKATSUKI
Senior Chief Researcher
Steel Research Dept.
Science & Technology Research Unit
Nippon Steel & Sumikin Research Institute Corporation

Kenji SORAO
Senior Manager
Personnel Dept.
R&D Laboratories

Koichiro TAKESHITA
Senior Manager, Head of Central Maintenance Dept.
Equipment Div.
Oita Works

Keishiro IKEDA
Senior Manager
Plate Technical Dept.
Plate Div.
Oita Works

Daisuke NAKAGAWA
Manager, Head of Section
Plate Mill
Plate Div.
Oita Works